

Discovery prospects with the Dark-photons & Axion-Like particles Interferometer —part I

Javier De Miguel*

*The Institute of Physical and Chemical Research (RIKEN),
Center for Advanced Photonics, 519-1399 Aramaki-Aoba, Aoba-ku, Sendai, Miyagi 980-0845, Japan*†

Juan F. Hernández-Cabrera

*Instituto de Astrofísica de Canarias, E-38200 La Laguna, Tenerife, Spain and
Departamento de Astrofísica, Universidad de La Laguna, E-38206 La Laguna, Tenerife, Spain*

On behalf of the DALI Collaboration

(Dated: March 27, 2023)

We discuss the discovery potential of the Dark-photons & Axion-Like particles Interferometer (DALI) in this letter. The apparatus, currently in a prototyping phase, will scan for Galactic axion dark matter from the Teide Observatory, an environment protected from terrestrial microwave sources, reaching Dine–Fischler–Srednicki–Zhitnitsky-like axion sensitivity in the range 25–250 μeV of mass, with a capacity to probe also dark sector photons of kinetic mixing strength in excess of several 10^{-16} ; or to establish new constraints to the stochastic gravitational wave background in this band. We identify different branches, including cosmology, stellar and particle physics, where this next-generation halo-telescope may represent a turning point in coming decades thanks to a powerful, cost-effective and technologically affordable experimental approach.

I. INTRODUCTION

Non-luminous, ‘dark’ matter is thought to play an important role in galactic dynamics, the halos of spiral galaxies being benchmark astronomical laboratories [1–3]. Paralleled, the current picture in cosmology suggests that a cosmological constant, Λ , and cold dark matter (CDM), enormously influence the evolution of the universe. A highly accelerated inflationary expansion during a brief cosmological timeframe, and the cosmic microwave background (CMB), also shape the Λ CDM model [4–10]. Large scale observations, simulations and the anisotropy measured in the CMB seem agreed in indicating the existence of CDM to favour the formation of the structures observed in the contemporary cosmos [11–23].

The quantum chromodynamics (QCD) axion is a long-postulated pseudo-scalar boson that arises as a consequence of the dynamic solution to the charge and parity (CP) symmetry problem in the strong interaction [24–26]. Furthermore, axion can simultaneously solve the dark matter enigma in a broad coupling strength to photons, $g_{a\gamma\gamma}$, to axion mass, m_a , parameter space [27–30]. Moreover, beyond shaping galaxies by forming halos, the primordial density perturbations from which galaxies evolved may have been produced by the presence of temporary axion domain walls in the early Universe [31]. Indeed, approaches have been proposed that

simultaneously solve the strong CP problem, axion dark matter and inflation in an unique model [32–36]. On the other hand, astronomical observations and simulations have given rise to the conjecture that dark matter in the nearby Universe is distributed in the form of sub-structures, which would produce an observable imprint on the electromagnetic spectrum [37–43]. Lastly, a series of anomalous astronomical observations have led to hypothesize that new physics may act as a factor in determining the precise details of stellar evolution [44–47].

All of the above encourages the quest for axion-like dark matter as a *nomos* of modern physics. The search for dark matter by axion-photon interaction is, in particular, promising. Laboratory experiments have excluded the sector $g_{a\gamma\gamma} \gtrsim 10^{-7} \text{ GeV}^{-1}$ for $m_a \lesssim 10^{-3} \text{ eV}$ [48–51]. Helioscopes, partially overlapping stellar hints based on interactions of the axion to standard particles in the plasma of stars, exclude $g_{a\gamma\gamma} \gtrsim 10^{-10} \text{ GeV}^{-1}$ for $10^{-2} \lesssim m_a/\text{eV} \lesssim 10^5$ [52]. Different astronomical campaigns and simulations rule out distinct parameter spaces [53–58]; while cosmogony also restricts the mass of this pseudo-Goldstone boson to allow the structures observed in the contemporary Universe to be formed in a CDM picture and, as a result, the search for axion in the range $10^{-6} \lesssim m_a/\text{eV} \lesssim 10^{-3}$ is well motivated [30, 59].

The velocity dispersion of Halo dark matter is about $10^{-3}c$, with c the speed of light and, therefore, relativistic corrections are negligible and the dynamic and rest mass of the particles coincide; the wavelength of electromagnetic radiation emitted is $\omega \sim m_a$ in consequence. Axion being a significant component of Halo dark matter, on the order of millions of axion-to-photon oscillation events per unit of time occur in the vessel of haloscopes,

* javier.miguelhernandez@riken.jp

† Also at Instituto de Astrofísica de Canarias,
E-38200 La Laguna, Tenerife, Spain

magnetised detectors equipped with resonators and microwave receivers which scan for the photons originating from the conversion, which represents a potent channel for the direct detection of Galactic axion [60]. This is the experimental approach to which we will confine our attention throughout this work, which is, however, also sensitive to dark photon, an alternative candidate to dark matter, via kinetic mixing [61, 62]; and to high-frequency gravitational waves, within a faint parameter space determined by the Planck scale, through photon-graviton oscillation in an external magnetic field [63–68].

The letter is structured as follows. In Sec. II we overview the experimental set-up of DALI experiment. Section III is devoted to examine its potential for discovering new physics. Conclusions are recapitulated in Sec. IV.

II. EXPERIMENTAL APPROACH

The quest for axion at masses below a few dozen microelectronvolt has been performed by conventional haloscopes for decades [69–74]. Unfortunately, the search for axion at ‘high frequency,’ above, say, two dozen micro-electronvolt of mass or, equivalently, about half a dozen gigahertz, remains poorly explored as those classical detectors, based on the resonant-cavity working principle, require movable components which become nonoperational when cryogenised in strongly magnetised cylindrical cavities with a diameter below a few centimeters, and narrower as the axion mass increases, since its size scales as $d \sim c/\nu_0$; with d the diameter, ν_0 the resonant frequency at which axion is probed.

In contrast, the operational principle of DALI is based on the interferometry technique, addressing a Fabry–Pérot resonator composed of dielectric plates instead of a resonant cavity [75–77]. As long as the integral of the axion wave function over consecutive layers does not vanish, higher order modes play a role in axion-to-photon conversion while the amplitude of the enhancement factor is increased by resonance. Interestingly, since the resonant frequency is tuned by setting a wavelength fraction of distance between the dielectric layers causing a constructive interference by reflection off a top mirror, the tuning results independent of the size, provided the plate scale length is larger than the wavelength to avoid diffraction, rendering axion scanning possible in heavier masses. The output is spectrally modified compared to the input beam around a central frequency, enabling axion detection in a reasonable integration time within a broad mass range [78–80]. The DALI concept is shown in Fig. 1, and detailed in more depth in [77].

A highly sensitive DALI instrument requires to maximize the cross-sectional area of detection, via a large magnet bore; the power enhancement factor, more importantly, through a high number of layers, and, crucially, the external field strength, by incorporating a potent superconducting magnet. Niobium–titanium, NbTi, super-

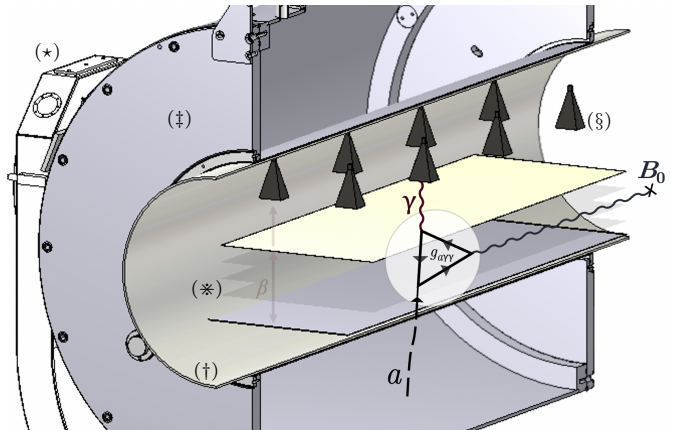


FIG. 1. DALI concept. The experiment cryostat,[†] cylindrical shape, is housed within the warm bore of a solenoid superconducting magnet[‡] and employs an independent ³He cooling system in order to provide a sub-kelvin background temperature. The dielectric layers, in yellow, are composed of wafers made of zirconia, ZrO_2 ; while a polished mirror is attached at the bottom to envelop the Fabry–Pérot interferometer providing the signal boost, β .^{*} The microwave signal, originating at an axion-photon-photon vertex, is received by an antenna array,[§] in black, and post-processed using radio-interferometry-like techniques [81, 82]. The apparatus rests on an altazimuth mount,[†] in white on the left, to provide the instrument with directionality. Overall dimensions are about two meters in length and one meter in diameter. Some objects have been removed for simplicity.

conductor does not provide magnetic field flux densities above 9–10 T when cooled down to a physical temperature of 4.2 K. Using more powerful, and demanding, cryogenic systems, NbTi can be, however, cooled down to 2 K, which renders field strengths of up to about 11.7 T feasible. In consequence, regular multicoil and solenoid magnets can present field strengths of 9.4 or 11.7 T with a warm bore of about 50–90 cm, from a few to several meters in length, and a field homogeneity several dozens parts per million over a few centimeters diameter of spherical volume. In occasions, niobium–tin, Nb_3Sn , is used to provide field strengths beyond 11.7 T, with a limit about, approximately, 23.5 T; although this superconductor material is, roughly, one order of magnitude more costly than NbTi and, therefore, its use is less widespread. Finally, high-temperature superconductors have been proposed to reach magnetic fields in excess of 23.5 T, although they are still at an early stage of development, while hybrid magnets are maturing that also far surpass the state of the art [83–85]. In this line of thought, a first, cost-effective phase using a superconducting solenoid working at 9.4 T is planned for the DALI Experiment, which we will refer to as phase I; followed by a second phase, of a larger scale, involving an up-grade to 11.7 T aimed at scanning with increased sensitivity those sectors for which there is a well-founded theoretical motivation. In both phases of the project only currently available technology is to be used as part of our strategy

to contribute an experiment with a high feasibility and readiness.

III. DISCOVERY POTENTIAL

In this section we look at the potential of DALI to unveil new physics.

A. CP symmetry and axion dark matter

The QCD Lagrangian density includes an angular term, which is read

$$\mathcal{L}_\theta = \frac{1}{32\pi^2} \theta G_{\mu\nu}^a \tilde{G}_{\mu\nu}^a, \quad (1)$$

where the gluon field strength is $G_{\mu\nu}^a$ and $\tilde{G}_{\mu\nu}^a$ its dual. We express natural units throughout this letter, except where indicated explicitly. To preserve CP symmetry in QCD, the θ term in Eq. 1, which allows for symmetry violation, is promoted to a field, with a Mexican hat potential that evolves towards a minimum as time advances in an early universe, in the most elegant explanation to date [24]. Oscillations give rise to particles, which have been termed ‘axion’ [25, 26]. The non-observation of a neutron electric dipole moment by modern experiments suggest that θ is negligibly small, at the level of $|\theta| < 10^{-10}$ and, consequently, CP symmetry would be preserved, in practice, at present [86, 87]. Axion interacts, weakly, with standard particles. The axion-photon interaction term is

$$\mathcal{L}_{a\gamma}^{\text{int}} = -\frac{1}{4} g_{a\gamma\gamma} F_{\mu\nu} \tilde{F}^{\mu\nu} a, \quad (2)$$

with $F^{\mu\nu}$ the photon field strength tensor and a the axion field. From a classic approach, Eq. 2 simplifies to $\mathcal{L}_{a\gamma}^{\text{int}} = g_{a\gamma\gamma} \mathbf{E} \cdot \mathbf{B} a$; \mathbf{E} being the photon field and \mathbf{B} a static magnetic field providing a virtual photon which enables the Primakoff effect at a axion-photon-photon vertex, $a + \gamma_{\text{virt}} \leftrightarrow \gamma$, in a polarization favored by the dot product [88].

The coupling rate of the QCD axion contains a factor derived from the ratio of electromagnetic and color anomalies, \mathcal{E}/\mathcal{C} , which reads $c_{a\gamma\gamma} = 1.92(4) - \mathcal{E}/\mathcal{C}$; with $c_{a\gamma\gamma} = -\frac{\alpha}{2\pi} g_{a\gamma\gamma} f_a$, α being the fine structure constant and f_a the axion field scale, giving the digit in parentheses accounts for the uncertainty. In the Kim–Shifman–Vainshtein–Zakharov (KSVZ) model, $\mathcal{E}/\mathcal{C} = 0$ and $\mathcal{C} = 1$ are adopted [89, 90]. In contrast, the Dine–Fischler–Srednicki–Zhitnitsky (DFSZ) axion adopts \mathcal{E}/\mathcal{C} equal 8/3—the so-called DFSZ I—or 2/3—DFSZ II—and \mathcal{C} equal to 6 or 3 [91, 92]. Differently from QCD axion models, for the so-called axion-like particles (ALPs), which arise in extensions of the Standard Model of particle physics, coupling to photons and mass are independent, resulting in a larger parameter space to be explored

[93, 94]. The main objective of DALI is to detect Galactic axion dark matter by inverse Primakoff. The haloscope is sensitive to axion-like particles with a coupling strength to photons

$$\begin{aligned} \frac{g_{a\gamma\gamma}}{\text{GeV}^{-1}} &\gtrsim 2.5 \times 10^{-13} \times \left(\frac{\text{SNR}}{\beta^2} \right)^{1/2} \\ &\times \left(\frac{m^2}{A} \right)^{1/2} \times \left(\frac{m_a}{\mu\text{eV}} \right)^{5/4} \times \left(\frac{s}{t} \right)^{1/4} \\ &\times \left(\frac{T_{\text{sys}}}{K} \right)^{1/2} \times \frac{T}{B_0} \times \left(\frac{\text{GeVcm}^{-3}}{\rho_a} \right)^{1/2}, \end{aligned} \quad (3)$$

where SNR is signal to noise ratio, β is boost factor, or signal enhancement originating from resonance, A is cross-sectional area, t is integration time and the system temperature is T_{sys} ; while B_0 is magnetic field strength

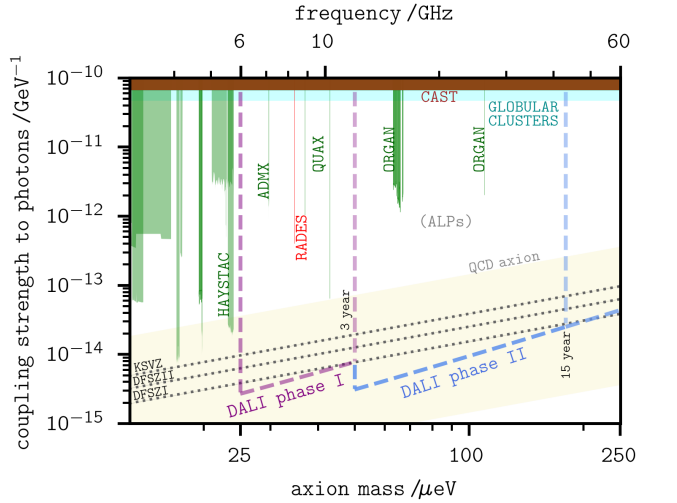


FIG. 2. A forecast of the sensitivity of DALI Experiment to Galactic axion projected onto current exclusion limits established by different means, differentiated by color [44–58, 69–74, 95–104]. The magnetic field density is 9.4 T or 11.7 T for phase I, in purple, and phase II, in blue, respectively; the cross-sectional plate area is 1/2 or 3/2 m², and 40–50 layers are incorporated to provide a power boost factor of the order of 10⁴ or higher. The system temperature is determined by a sub-kelvin background temperature provided by ³He coolers plus an offset contributed by the limit of heat dissipation in the electronics, roughly three times over the quantum noise limit, in order to be consistent with the frequency-dependent noise figure in high-electron-mobility transistor technology, with a physical temperature at the level of one kelvin, which causes a slope with respect to the QCD axion projections [105, 106]. The instantaneous scanning bandwidth is between several dozens to a few hundred megahertz; while the linewidth is $\Delta\nu/\nu \approx 5 \times 10^{-7}$. The KSVZ and DFSZ axion models are extended to the experimental range, 25–250 μeV . The QCD axion window shadowed in yellow is defined in [107]. Region in white is compatible with axion-like particles (ALPs).

and ρ_a is the density of axion-like dark matter in the laboratory.

In the light of the sensitivity projections in Fig. 2, it follows that DALI has a capacity to probe DFSZ I-type axion models between 25–50 μeV within approximately three years in the initial phase of the experiment. During phase II, sensitivity will be increased allowing DALI to scan for DFSZ I axion in the 50–180 μeV over a period of about three lustrums, and beyond.

We recompute the sensitivity of the system by means of a Monte Carlo simulation in the Supplemental Material accompanying this letter [108].

B. Other frontiers of knowledge are expanded

The search for and detection, or parametric constriction, of the axion can shed light on a number of problems in physics, as discussed in the following paragraphs.

1. Examining cosmology in a post-inflationary universe

The color anomaly is an integer referred to as ‘domain wall number,’ $\mathcal{N} \leftarrow \mathcal{C}$, in cosmology. On the other hand, hereinafter we will refer to the ‘phase transition’ as the moment in the history of the early Universe in which the axion angular field, θ , acquires propagating degrees of freedom and symmetry is broken. In a pre-inflationary scenario, in which the phase transition takes place before inflation, axion strings, domain walls, emerging if $\mathcal{N} > 1$, and their decay remnants, will be cleaned out by the expansion. In an universe in which symmetry breaking originates after inflation, domain walls would rapidly govern the density of energy, invoking catastrophic topological objects [59, 109, 110]. For axion models which adopt $\mathcal{N} = 1$, such as the KSVZ model, these topological defects are naturally avoided. In such a post-inflationary scenario, models with $\mathcal{N} > 1$, including the DFSZ axion, must, in contrast, circumvent those dramatic topological effects by alternative mechanisms [111–116].

The axion field is massless before the phase transition. Axion mass below, say, 20 μeV is more consistent in a pre-inflationary scenario, at which the axion mass takes a single value. The axion mass in a post-inflationary scenario, where different patches can present different misalignment angle when the phase transition begins, is, typically, restricted to the range $25 \mu\text{eV} \lesssim m_a \lesssim 1 \text{ meV}$ —cf. [30, 59, 117]. Recent studies even constrain the latter range further, to $40 \lesssim m_a/\mu\text{eV} \lesssim 180$, by means of a refinement of the cosmic string resolution, to which DALI will pay special attention [118].

It is worth mentioning that some efforts have been redirected to unify the strong CP problem, axion dark matter and cosmic inflation in an unique model, simultaneously solving other problems of modern physics that we will not deal with in this letter [32–36]. Seeking to be compatible with currently available observational

data, which in part modelled the ΛCDM cosmology, the parameter space of the simulations is accordingly constrained, yielding an axion mass of the order of $50 \lesssim m_a/\mu\text{eV} \lesssim 200$ [34], which DALI also matches.

From all of the above, it follows that axionic phase transition and cosmogony are closely related. The detection of axion within a parameter space which favours a specific axion model, or hypothesis, would shed light on the topology of strings, domain walls, and their evolution, examining cosmic inflation and its role in the evolution of the Universe and, more importantly perhaps, the standard cosmological model itself.

2. Astrophysical bounds of axion dark matter

Axions interact with fermions and photons in the plasma of stars, producing extra cooling. The confrontation of stellar evolution models, modified to account for the additional energy loss rate that axion scattering would cause, with observational data, allows to set limits to the coupling constants of the pseudoscalar with ordinary particles. A succinct review of the field concerns us. Accelerated consumption of helium reduces the stellar lifetime. Stars on the horizontal branch (HB) present accelerated burning rates that can be compared with the expected Primakoff axion loss rate. Thus, axion coupling to photons would reduce the lifetime of HB stars, while producing negligible changes on red giant (RG) branch (RGB) evolution as RGs are only weakly affected by the Primakoff effect. However, RGs suffer from axion coupling to electrons in several radiative processes, such as atomic axio-recombination or deexcitation, axion bremsstrahlung and Compton scattering. White dwarfs (WDs), where the Primakoff and Compton processes are suppressed by the plasma frequency, are, nevertheless, sensitive to bremsstrahlung. Photometry compared with WD luminosity function models can reveal additional cooling due to axion-induced losses. Furthermore, the neutrino flux duration from supernova (SN) SN1987A compared to numerical simulations of state-of-the-art SN models can also be used to constrain the parametric sector of the axion. Lastly, observations of the neutron star in the SN remnant Cassiopeia A disclose an abnormally fast cooling rate. This extra cooling could be explained by axion-neutron bremsstrahlung. Axion-like particles coupling to both electrons and photons would simultaneously be able to explain HB, RGB stars and WD extra cooling, in concordance with SN1987A and Cassiopeia A hints, which fosters the exploration of the corresponding sector with DFSZ axion sensitivity, that has never been achieved in the mass range we are concerned with in this letter [46, 119–130]. Remarkably, DALI has a potential to explore these astro-bounds, whose most restrictive limits within its band to date, set by the ratio of stars in HB over RGB—the so-called R parameter—and the ratio of stellar populations on the asymptotic giant

branch to HB in globular clusters—R₂—, are projected onto Fig. 2 [46, 122], with DFSZ I sensitivity. To end, we confer our care to the synergism with the astronomical exploration of the spectral feature that originates when ambient axions fall on neutron stars, appearing as a narrow emission line with a frequency corresponding to the axion mass by axion-photon resonance in the magnetised plasma of the magnetosphere, as a candidate could be confirmed or discarded with DALI by direct methods—see [131–133] and references therein.

3. Dark sector photons

Dark photon, also referred to as hidden photon or paraphoton, is a hypothetical gauge boson that mixes kinetically with ordinary photons [61, 62]. The interaction term relevant for this work reads

$$\mathcal{L}_{\gamma'\gamma}^{\text{int}} = -\frac{1}{2} F_{\mu\nu} \tilde{X}^{\mu\nu} \chi, \quad (4)$$

where we denote by $\tilde{X}^{\mu\nu}$ the field strength tensor of the dark photon field; χ being the, dimensionless, kinetic mixing strength.

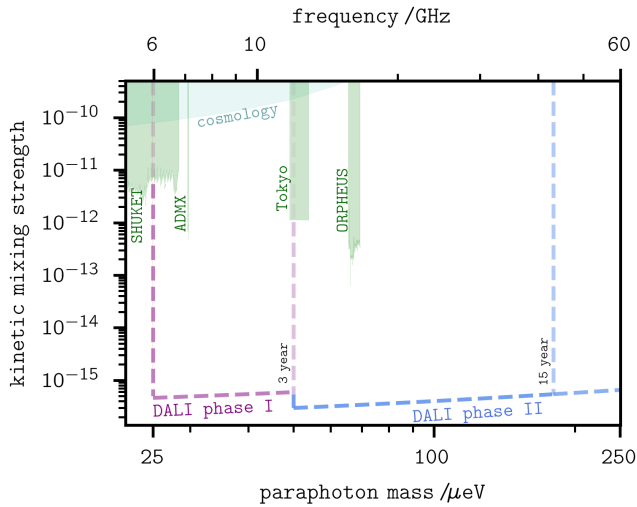


FIG. 3. Projection of the sensitivity of DALI to dark sector photon dark matter with overlapping boundaries published at the time of writing [134–140]. Sensitivity enhancement in a fixed polarisation scenario owing to an unrestricted directionality, suggested in [141], does not rescale in this plot.

Instrumental sensitivity to Galactic paraphotons reads

$$\chi \gtrsim 2.9 \times 10^{-14} \times \left(\frac{\text{SNR}}{\beta^2} \right)^{1/2} \times \left(\frac{m^2}{A} \right)^{1/2} \times \left(\frac{\Delta\nu}{\text{Hz}} \right)^{1/4} \times \left(\frac{s}{t} \right)^{1/4} \times \left(\frac{T_{\text{sys}}}{K} \right)^{1/2} \times \left(\frac{\text{GeVcm}^{-3}}{\rho_{\gamma'}} \right)^{1/2} \times \frac{\sqrt{2/3}}{\alpha}, \quad (5)$$

$\alpha = \sqrt{2/3}$ representing random incidence angle of the dark photon [142]. Hidden photons being most of Galactic dark matter, a forecast of DALI sensitivity is depicted on Fig. 3.

4. Exploration of a dark universe

Different patches, causally disconnected as a result of a scenario at which the phase transition takes place after cosmic inflation, could favour the formation of substructures of axion dark matter [143]. If a substructure were to traverse our planet, it would induce a measurable imprint on the electromagnetic spectrum modulated by celestial mechanics. Substructures have been shown to approach the Solar System by analyzing survey data, with event rate that may not be insignificant [144–146]. DALI incorporates an altazimuth mount which enhances its sensitivity to dark matter flows and streams passing through the Earth's position. The daily signal modulation caused by a collision with a substructure made of axion-like particles, or paraphotons, can be expressed in terms of the modulation parameters c_0, c_1 and ϕ , in the form $c_0 + c_1 \cos(2\pi t/0.997 + \phi)$; t being the time expressed in days from January 1st, and

$$\begin{aligned} & c_0^N \\ & b_0 \cos \lambda_{\text{lab}} - b_1 \sin \lambda_{\text{lab}} \cos(\omega_d t + \phi_{\text{lab}} + \psi), \end{aligned} \quad (6a)$$

$$\begin{aligned} & c_1^W \\ & b_1 \cos(\omega_d t + \phi_{\text{lab}} + \psi - \pi), \end{aligned} \quad (6b)$$

$$\begin{aligned} & c_0^Z \\ & b_0 \sin \lambda_{\text{lab}} + b_1 \cos \lambda_{\text{lab}} \cos(\omega_d t + \phi_{\text{lab}} + \psi), \end{aligned} \quad (6c)$$

where $b_0 = \sigma_3 |V_{\text{lab}} - V_a|^{-1}$, $b_1 = (\sigma_1^2 + \sigma_2^2)^{1/2} |V_{\text{lab}} - V_a|^{-1}$, $\psi = \tan^{-1}(\sigma_1/\sigma_2) - 0.721\omega_d - \pi/2$; $\sigma_1 = (-0.055, 0.494, -0.868) \cdot \Upsilon$, $\sigma_2 = (-0.873, -0.445, -0.198) \cdot \Upsilon$, $\sigma_3 = (-0.484, 0.747, 0.456) \cdot \Upsilon$, with $\Upsilon = V_{\odot} + v_{\oplus} \cos(\tau_y)(0.994, 0.109, 0.003) + v_{\oplus} \sin(\tau_y)(-0.052, 0.494, -0.868)$, $\tau_y = 2\pi(t - 79)/365$ [77, 145].

The simulation of an event is shown in Fig. 4. Interestingly, the search for Halo axions and substructures can be performed simultaneously, analyzing the data in search of a periodisation. Detection of this trace would support the hypothesis of dark matter substructures navigating in a ‘dark universe’ [37–43].

C. Peripheral objectives of the project

1. Examining axion quark nugget theory

The quest for axion quark nuggets (AQNs) deserves a separate mention. Those relic specks were postulated to explain the observed density ratio between non-luminous and visible matter, $\Omega_{\text{dark}}/\Omega_{\text{visible}} \sim 1$, regardless of initial

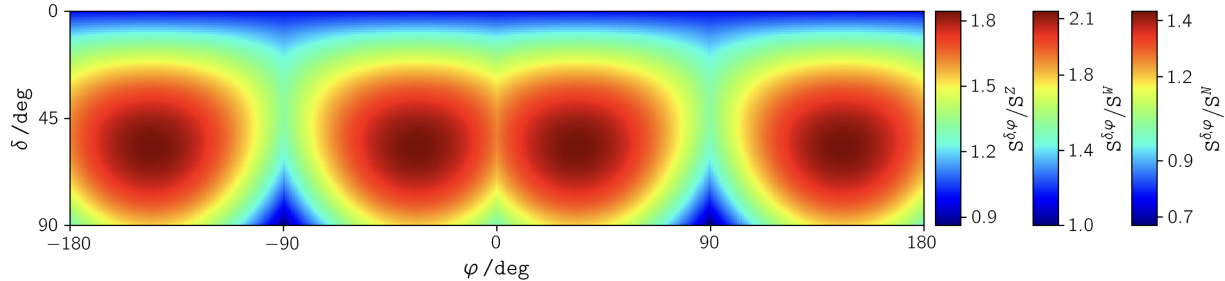


FIG. 4. Significance of the signal modulation $S^{\delta, \varphi}$, for a collision with a substructure composed of axion-like dark matter, compared to the signal modulation significance of a zenith, north or west pointing experiment, $S^{Z, N, W}$. The inclination angle measured from the fixed zenith direction is δ ; φ is the azimuth angle of its orthogonal projection on a north-west plane, from the north fixed reference. A west-pointing haloscope does not account for the parameter c_0 . The telescope is bidirectional. The optimal pointing varies with lab coordinates and the period. Observed in the Teide Observatory, Canary Islands, during the first day of the year. The result, in normalised sigma units, is independent from axion model and mass, substructure density, velocity and dispersion.

misalignment angle or axion mass, in a $\mathcal{N} = 1$ scenario [147, 148]. The sensitivity of a DALI-like device to axions released by AQNs is read

$$\frac{g_{a\gamma\gamma}}{\text{GeV}^{-1}} \gtrsim 2.1 \times 10^{-7} \times \left(\frac{\text{SNR}}{\beta^2(v_a)} \right)^{1/2} \times \left(\frac{m^2}{A_s} \right)^{1/2} \times \left(\frac{m_a}{\mu\text{eV}} \right)^{5/4} \times \left(\frac{s}{t} \right)^{1/4} \times \left(\frac{T_{\text{sys}}}{\text{K}} \right)^{1/2} \times \frac{T}{B_0} \quad (7)$$

$$\times \left(\frac{\text{eVcm}^{-3}}{\rho_{v_a}^{\text{AQN}}} \right)^{1/2} \times \left(\frac{v_a}{c} \right)^{1/2} \times \frac{1}{\sqrt{n}}.$$

A scaled-down, same DALI concept, parasitic detector devoted to the exploration of terrestrial axion flux induced by AQNs can be brought to a practical realization. Such an array of n independent pixels would have a smaller plate scale, s , on the order of a dozen centimeters to maintain de Broglie coherence, which would give the prototype access to relativistic axions of up to, roughly, one hundred microelectronvolt of mass [77], with a cut-off near $c/5$ —note that the spectral density function of AQN-induced axions peaks around $c/2$. From [149, 150] it follows that the fluence of semi-relativistic axion on Earth originating from collisions with those macroscopic specs is, approximately, $\Phi_{v_a < 0.2c}^{\text{AQN}} \sim 10^{12} \text{cm}^{-2}\text{s}^{-1}(\text{eV}/m_a)$, which results in an occupancy of about $\rho_{v_a < 0.2c}^{\text{AQN}} \sim 10^2 \text{eVcm}^{-3}$, that is, several orders less concentrated than the saturation density of dark matter at the position of the Solar System, about $\text{few} \times 10^8 \text{ eVcm}^{-3}$. However, recent work has pointed out that a gravitationally focused stream of AQNs could transiently increase the occurrence of annihilation events by a factor of up to 10^6 [151]. Notwithstanding that the semi-relativistic velocities, $v_a \lesssim 0.2c$, of those axions would decrease the signal boost factor [152], a partially resonant, not purely transparent, harmonically hybrid mode could take advantage of the larger momentum transmitted by the rapid axions to the dielectric layers

of the resonator and allow one to maintain, or perhaps increase, the power enhancement, $\beta^2(v_a)$, with respect to the zero-velocity limit boost that can be achieved for slower axions that form the halo of the Milky Way. In addition, signal modulation caused by celestial mechanics, and the so-called ‘local-flashes,’ bursts resulting from the interaction of AQNs with the Earth in the vicinity of a detector, could be accounted for by an amplification parameter with typical magnitude 10^{2-4} during a short period of time with a non-negligible event rate [149, 150]. The sensitivity is multiplied by $[(v_a/c)^2/10^{-6}]^{1/4}$ on the right-hand side of Eq. 7 to give account on the broadening and subsequent dilution of the signal in frequency domain which is caused by the semi-relativistic velocity of the AQN-induced axions compared to that of virialized particles. However, the above aspects, separately or together, can give the instrument access to the KSVZ axion window.

In fact, Eq. 7 can be transferred to any exotic source of semi-relativistic axion astroparticles—e.g., the explanation for the intriguing Antarctic Impulse Transient Antenna (ANITA) events [153, 154] in [155].

2. Constraints on the diffuse gravitational wave background

Graviton, the gravitational wave (GW) counterpart in the form of a long-postulated elementary particle, mix with photons in the presence of static magnetic fields [65, 156, 157]. The Lagrangian density of the interaction is

$$\mathcal{L}_{g\gamma}^{\text{int}} = -\frac{1}{2} \kappa h_{\mu\nu} B^\mu B^\nu, \quad (8)$$

where the gravitational coupling is $\kappa^2 = 16\pi m_{\text{Pl}}^{-2}$, with $m_{\text{Pl}} \sim 10^{19} \text{ GeV}$ the Planck mass; $h_{\mu\nu}$ denotes the graviton, B^μ is the external magnetic field and B^ν the electromagnetic wave. The mechanism is favored when the

external magnetic field is perpendicular to the direction of photon propagation [158].

Standard cosmology predicts a gravitational wave background (GWB) generated by a series of processes in the primitive Universe; with a contribution from astronomical sources. Irreducible emission from the time evolution of the momentum-energy tensor and cosmic string decay, the coalescence of primordial black hole (PBH) binaries and the evaporation of low-mass PBHs, branes oscillation, or those of astrophysical origin, such as solar thermal gravitational waves, supernova collapse, rotating neutron stars, binary systems, etc., contribute to shape a diffuse GWB [159–164].

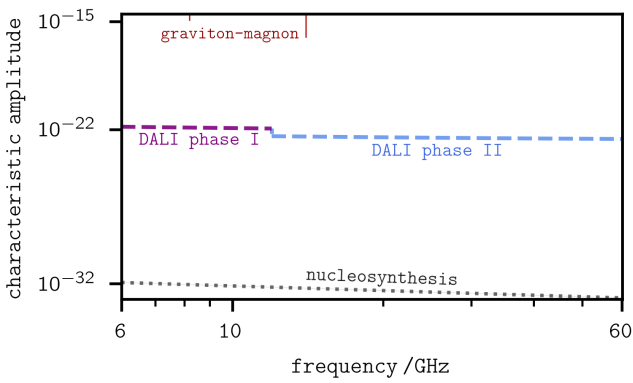


FIG. 5. Accessible characteristic amplitude of a high-frequency stochastic and isotropic gravitational wave background. Results overlapping the experimental range, from [165], are plotted in red.

In the spirit of [160], we introduce the, dimensionless, characteristic amplitude, $h_c = (6\Omega_{\text{GW}})^{1/2}H_0\omega^{-1}$; with $\Omega_{\text{GW}}(\omega)$ the spectral density function of a stochastic GWB, H_0 the Hubble parameter, ω the pulse of the wave. Primordial gravitational waves contribute to the density of species during nucleosynthesis as massless neutrinos, which results in a higher freezing temperature at which expansion breaks the $pe \leftrightarrow nv_e$ equilibrium; thus affecting the baryon to photon ratio that can be observed to constrain the cosmic GWB, to $h_c \lesssim 4.5 \times 10^{-22} \text{ Hz}/\omega$, within the framework of the cosmological model.

Unfortunately, the cross-section of the photon-graviton oscillation triggered by an external magnetic field involves energy level at the Planck scale, with an oscillation probability weighted by m_{Pl}^{-2} and, therefore, the direct detection of the high-frequency GWB through this mechanism cannot be tackled with technology currently within human reach. Some experiments have, in any case, exploited the weak coupling of the graviton to ordinary particles to set bounds to the amplitude of the GWB at shorter wavelengths. Interferometers have established $h_c \gtrsim 10^{-18}$ at 1 MHz, $h_c \gtrsim 10^{-19}$ at 13 MHz and $h_c \gtrsim 10^{-10} - 10^{-12}$ at 100 MHz [166–169]; while the graviton-magnon resonance detector in [165] establishes $h_c \gtrsim 10^{-15}$ at around 8 GHz and $h_c \gtrsim 10^{-16}$ at 14 GHz.

The analysis carried out in [164] using data from light-shining-through-wall experiments in [170, 171], and helioscopes [52], establishes upper bounds $h_c \gtrsim 10^{-25}$ and $h_c \gtrsim 10^{-25}$ at 10^{14-15} Hz; and $h_c \gtrsim 10^{-27}$ at around 10^{18} Hz. Appealingly, DALI can set the most restrictive experimental constraints to the amplitude of the high-frequency GWB in its band, via graviton-to-photon conversion in the magnetic chamber. Inspired by the concept outlined in [164, 172], it is possible to infer the minimum amplitude of a stochastic GWB that can be detected

$$h_c \gtrsim 9.2 \times 10^{-12} \times \left(\frac{\text{SNR}}{\beta^2} \right)^{1/2} \times \left(\frac{m^2}{A} \right)^{1/2} \times \left(\frac{\text{Hz}}{\nu} \right)^{1/2} \times \left(\frac{s}{t} \right)^{1/4} \times \left(\frac{\text{Hz}}{\Delta\nu} \right)^{1/4} \times \left(\frac{T_{\text{sys}}}{K} \right)^{1/2} \times \frac{T}{B_0} \times \frac{m}{L}, \quad (9)$$

where L is the magnetised length of flight; which is projected onto Fig. 5.

IV. CONCLUSIONS

The discovery potential of DALI for unveiling new physics is summarised in Table I. Although the scientific objectives of this experiment are, in some way, puzzling and superimposed, distinction is attainable. By ramping the magnet on/off it would be possible to differentiate between axion-like and dark photon dark matter; while the contribution of nucleosynthesis to an isotropic and stochastic gravitational wave background, on the other hand, would manifest itself as a signal that would not be detuned in small frequency steps. Collision with substructures, in turn, would present a peculiar modulation and a shortened duration; while the spectral feature originated by AQN-induced axions would also have properties that would allow it to be discriminated. This renders the project ends practicable.

In future articles we will delve into more unsolved problems in present-day physics in which DALI could play a decisive role.

ACKNOWLEDGEMENTS

The work of J.D.M. was supported by RIKEN's program for Special Postdoctoral Researchers (SPDR); J.F.H.C. is supported by the Resident Astrophysicist Programme of the Instituto de Astrofísica de Canarias (IAC). We gratefully acknowledge financial support from the Severo Ochoa Program for Technological Projects and Major Surveys 2020-2023 under Grant No. CEX2019-000920-S; Recovery, Transformation and Resiliency Plan of Spanish Government under Grant No. C17.I02.CIENCIA.P5; FEDER operational programme under Grant No. EQC2019-006548-P; IAC Plan de Actuación 2022. We thank the following members of the DALI Collaboration, and other colleagues, for dis-

TABLE I. Discovery potential of DALI. Recap of the core and peripheral project goals discussed throughout this letter. Axion detection refers to the first third, dark photon physics to the second inset, upper limits to a gravitational wave background follow the last horizontal line. Sensitivity is expressed in terms of $g_{a\gamma\gamma}$, by means of a fiducial model, KSVZ or DFSZ, for axion; kinetic mixing constant, χ , for paraphoton; characteristic amplitude of a stochastic gravitational wave background, h_c , for graviton. The most remarkable impacts of this research are noted.

Branch and purpose	Band	Sensitivity	Impact
Charge&parity (CP) symmetry	25–250 μeV	DFSZ I	Strong CP problem in quantum chromodynamics washed ^a
Galactic axion-like dark matter	25–250 μeV	DFSZ I	Direct detection of dark matter; physics realignment ^b
ΛCDM cosmology (inflation)	40–180 μeV	DFSZ I	Heavier axion sustains cosmic inflation ^c
SMASH-type cosmology	50–200 μeV	>KSVZ	Standard model axion seesaw Higgs portal inflation (SMASH) test ^d
Dark universe (substructures)	25–250 μeV	DFSZ I	Dark matter agglomerates anisotropically in macroscopic structures ^e
Stellar evolution (cooling rate)	25–250 μeV	DFSZ I	Fine-tuning of star model (HB, RGB, WDs, ...) ^f
Axion quark nugget hypothesis	25–80 μeV	KSVZ	Dark matter detection; domain wall number set $\mathcal{N} = 1$ ^g
Dark photon dark matter	25–250 μeV	$\chi \sim 5 \times 10^{-16}$	Dark matter detection; Standard Model of particle physics extends ^h
Gravitational wave background	6–60 GHz	$h_c \sim 10^{-22}$	Bounds to big bang nucleosynthesis by a direct detection method ⁱ

^a Quantum chromodynamics solution to the so-called strong CP problem; a new pseudo-scalar added after the Higgs boson [173–175].

^b If ALPs are found a significant part of dark matter, cosmology and halo modeling, among other issues, may undergo fine adjustment.

^c Observation of axion of mass heavier than several dozens of microelectronvolts would support a post-inflationary scenario.

^d The SMASH window may add three right-handed neutrinos, one Dirac fermion, a new complex singlet scalar [34].

^e Detection of a daily signal modulation can involve large substructures, affecting cosmology, large-scale structure, clusters, galaxies, etc.

^f Confirmation of axion would allow fine-tuning of helium consumption rates; and conversely [46, 122].

^g AQNs set domain wall number, suggests on decay of topologicals, solar ultraviolet radiation excess, ‘primordial lithium puzzle’ [150].

^h If this alternative candidate for dark matter is detected, a dark sector would be added to the Standard Model of particle physics.

ⁱ More incisive experimental limits to the stochastic gravitational wave background provide useful information about the early Universe.

cussions; E. Joven-Álvarez, J. A. Rubiño-Martín, C.

Otani, E. Hernández-Suárez, R. Hoyland, R. Rebolo, H. Lorenzo-Hernández, K. Zioutas and A. Zhitnitsky.

[1] F. Zwicky, Die Rotverschiebung von extragalaktischen Nebeln, *Helvetica Physica Acta* **6**, 110 (1933).

[2] V. C. Rubin and J. Ford, W. Kent, Rotation of the Andromeda Nebula from a Spectroscopic Survey of Emission Regions, *Astrophys. J.* **159**, 379 (1970).

[3] G. Bertone and D. Hooper, History of dark matter, *Reviews of Modern Physics* **90**, 045002 (2018), arXiv:1605.04909 [astro-ph.CO].

[4] R. H. Dicke, P. J. E. Peebles, P. G. Roll, and D. T. Wilkinson, Cosmic Black-Body Radiation., *Astrophys. J.* **142**, 414 (1965).

[5] A. A. Penzias and R. W. Wilson, A Measurement of Excess Antenna Temperature at 4080 Mc/s., *Astrophys. J.* **142**, 419 (1965).

[6] A. A. Starobinsky, A New Type of Isotropic Cosmological Models Without Singularity, *Phys. Lett. B* **91**, 99 (1980).

[7] A. H. Guth, The Inflationary Universe: A Possible Solution to the Horizon and Flatness Problems, *Phys. Rev. D* **23**, 347 (1981).

[8] A. D. Linde, A New Inflationary Universe Scenario: A Possible Solution of the Horizon, Flatness, Homogeneity, Isotropy and Primordial Monopole Problems, *Phys. Lett. B* **108**, 389 (1982).

[9] A. Albrecht and P. J. Steinhardt, Cosmology for Grand Unified Theories with Radiatively Induced Symmetry Breaking, *Phys. Rev. Lett.* **48**, 1220 (1982).

[10] G. F. Smoot *et al.* (COBE), Structure in the COBE differential microwave radiometer first year maps, *Astrophys. J. Lett.* **396**, L1 (1992).

[11] G. R. Blumenthal, S. Faber, J. R. Primack, and M. J. Rees, Formation of galaxies and large-scale structure with cold dark matter, *Nature* **311**, 517 (1984).

[12] M. Davis, G. Efstathiou, C. S. Frenk, and S. D. White, The evolution of large-scale structure in a universe dominated by cold dark matter, *The Astrophysical Journal* **292**, 371 (1985).

[13] A. Klypin, J. Holtzman, J. Primack, and E. Regos, Structure Formation with Cold plus Hot Dark Matter, *Astrophys. J.* **416**, 1 (1993), arXiv:astro-ph/9305011 [astro-ph].

[14] A. R. Liddle and D. H. Lyth, The cold dark matter density perturbation, *Physics Reports* **231**, 1 (1993).

[15] L. Hernquist, N. Katz, D. H. Weinberg, and J. Miralda-Escude, The lyman-alpha forest in the cold dark matter model, *The Astrophysical Journal* **457**, L51 (1996).

[16] S. Galli, F. Iocco, G. Bertone, and A. Melchiorri, Cmb constraints on dark matter models with large annihilation cross section, *Phys. Rev. D* **80**, 023505 (2009).

[17] W. Hu, Mapping the dark matter through the cosmic microwave background damping tail, *The Astrophysical Journal* **557**, L79 (2001).

[18] D. N. Spergel and P. J. Steinhardt, Observational evidence for self-interacting cold dark matter, *Physical review letters* **84**, 3760 (2000).

[19] W. Hu and S. Dodelson, Cosmic microwave background anisotropies, *Annual Review of Astronomy and Astrophysics* **40**, 171 (2002),

<https://doi.org/10.1146/annurev.astro.40.060401.093926>.

[20] S. Alam *et al.* (BOSS), The clustering of galaxies in the completed SDSS-III Baryon Oscillation Spectroscopic Survey: cosmological analysis of the DR12 galaxy sample, *Mon. Not. Roy. Astron. Soc.* **470**, 2617 (2017), arXiv:1607.03155 [astro-ph.CO].

[21] Y. Wang, G.-B. Zhao, C.-H. Chuang, M. Pellejero-Ibanez, C. Zhao, F.-S. Kitaura, and S. Rodriguez-Torres, The clustering of galaxies in the completed SDSS-III Baryon Oscillation Spectroscopic Survey: a tomographic analysis of structure growth and expansion rate from anisotropic galaxy clustering, *Mon. Not. Roy. Astron. Soc.* **481**, 3160 (2018), arXiv:1709.05173 [astro-ph.CO].

[22] N. I. Libeskind *et al.*, Tracing the cosmic web, *Mon. Not. Roy. Astron. Soc.* **473**, 1195 (2018), arXiv:1705.03021 [astro-ph.CO].

[23] Planck Collaboration, Planck 2018 results. VI. Cosmological parameters, *Astronomy & Astrophysics* **641**, A6 (2020), arXiv:1807.06209 [astro-ph.CO].

[24] R. D. Peccei and H. R. Quinn, CP conservation in the presence of pseudoparticles, *Phys. Rev. Lett.* **38**, 1440 (1977).

[25] S. Weinberg, A new light boson?, *Phys. Rev. Lett.* **40**, 223 (1978).

[26] F. Wilczek, Problem of strong p and t invariance in the presence of instantons, *Phys. Rev. Lett.* **40**, 279 (1978).

[27] L. Abbott and P. Sikivie, A cosmological bound on the invisible axion, *Physics Letters B* **120**, 133 (1983).

[28] M. Dine and W. Fischler, The not-so-harmless axion, *Physics Letters B* **120**, 137 (1983).

[29] J. Preskill, M. B. Wise, and F. Wilczek, Cosmology of the invisible axion, *Physics Letters B* **120**, 127 (1983).

[30] Particle Data Group, Review of particle physics, *Phys. Rev. D* **98**, 030001 (2018).

[31] P. Sikivie, Axions, domain walls, and the early universe, *Phys. Rev. Lett.* **48**, 1156 (1982).

[32] A. Salvio, A Simple Motivated Completion of the Standard Model below the Planck Scale: Axions and Right-Handed Neutrinos, *Phys. Lett. B* **743**, 428 (2015), arXiv:1501.03781 [hep-ph].

[33] G. Ballesteros, J. Redondo, A. Ringwald, and C. Tamarit, Standard model—axion—seesaw—higgs portal inflation. five problems of particle physics and cosmology solved in one stroke, *Journal of Cosmology and Astroparticle Physics* **2017** (08), 001.

[34] G. Ballesteros, J. Redondo, A. Ringwald, and C. Tamarit, Unifying inflation with the axion, dark matter, baryogenesis, and the seesaw mechanism, *Physical review letters* **118**, 071802 (2017).

[35] A. Ernst, A. Ringwald, and C. Tamarit, Axion predictions in $so(10) \times u(1)$ pq models, *Journal of High Energy Physics* **2018**, 1 (2018).

[36] G. Ballesteros, J. Redondo, A. Ringwald, and C. Tamarit, Several Problems in Particle Physics and Cosmology Solved in One SMASH, *Frontiers in Astronomy and Space Sciences* **6**, 55 (2019), arXiv:1904.05594 [hep-ph].

[37] C. Hogan and M. Rees, Axion miniclusters, *Physics Letters B* **205**, 228 (1988).

[38] B. Moore, S. Ghigna, F. Governato, G. Lake, T. Quinn, J. Stadel, and P. Tozzi, Dark matter substructure within galactic halos, *The Astrophysical Journal* **524**, L19 (1999).

[39] J. Diemand, M. Kuhlen, P. Madau, M. Zemp, B. Moore, D. Potter, and J. Stadel, Clumps and streams in the local dark matter distribution, *Nature* **454**, 735 (2008).

[40] M. Vogelsberger and S. D. M. White, Streams and caustics: the fine-grained structure of a cold dark matter haloes, *Monthly Notices of the Royal Astronomical Society* **413**, 1419 (2011), arXiv:1002.3162 [astro-ph.CO].

[41] P. Tinyakov, I. Tkachev, and K. Zioutas, Tidal streams from axion miniclusters and direct axion searches, *Journal of Cosmology and Astroparticle Physics* **2016** (1), 035, arXiv:1512.02884 [astro-ph.CO].

[42] G. C. Myeong, N. W. Evans, V. Belokurov, N. C. Amorisco, and S. E. Koposov, Halo substructure in the SDSS-Gaia catalogue: streams and clumps, *Monthly Notices of the Royal Astronomical Society* **475**, 1537 (2018), arXiv:1712.04071 [astro-ph.GA].

[43] A. Vaquero, J. Redondo, and J. Stadler, Early seeds of axion miniclusters, *Journal of Cosmology and Astroparticle Physics* **2019** (04), 012.

[44] A. Ayala, I. Domínguez, M. Giannotti, A. Mirizzi, and O. Straniero, Revisiting the Bound on Axion-Photon Coupling from Globular Clusters, *Phys. Rev. Lett.* **113**, 191302 (2014), arXiv:1406.6053 [astro-ph.SR].

[45] O. Straniero, A. Ayala, M. Giannotti, A. Mirizzi, and I. Domínguez, Axion-Photon Coupling: Astrophysical Constraints, in *11th Patras Workshop on Axions, WIMPs and WISPs* (2015) pp. 77–81.

[46] M. J. Dolan, F. J. Hiskens, and R. R. Volkas, Advancing globular cluster constraints on the axion-photon coupling, *Journal of Cosmology and Astroparticle Physics* **2022** (10), 096, arXiv:2207.03102 [hep-ph].

[47] L. Di Luzio, M. Fedele, M. Giannotti, F. Mescia, and E. Nardi, Stellar evolution confronts axion models, *Journal of Cosmology and Astroparticle Physics* **2022** (2), 035, arXiv:2109.10368 [hep-ph].

[48] K. Ehret, M. Frede, S. Ghazaryan, M. Hildebrandt, E.-A. Knabbe, D. Kracht, A. Lindner, J. List, T. Meier, N. Meyer, D. Notz, J. Redondo, A. Ringwald, G. Wiedemann, and B. Willke, New alps results on hidden-sector lightweights, *Physics Letters B* **689**, 149 (2010).

[49] M. Betz, F. Caspers, M. Gasior, M. Thumm, and S. W. Rieger, First results of the cern resonant weakly interacting sub-ev particle search (crows), *Phys. Rev. D* **88**, 075014 (2013).

[50] F. Della Valle, A. Ejlli, U. Gastaldi, G. Messineo, E. Milotti, R. Pengo, G. Ruoso, and G. Zavattini, The PVLAS experiment: measuring vacuum magnetic birefringence and dichroism with a birefringent Fabry-Perot cavity, *European Physical Journal C* **76**, 24 (2016), arXiv:1510.08052 [physics.optics].

[51] R. Ballou, G. Deferne, M. Finger, M. Finger, L. Flekova, J. Hosek, S. Kunc, K. Macuchova, K. A. Meissner, P. Pugnat, M. Schott, A. Siemko, M. Slunecka, M. Sulc, C. Weinsheimer, and J. Zicha (OSQAR Collaboration), New exclusion limits on scalar and pseudoscalar axion-like particles from light shining through a wall, *Phys. Rev. D* **92**, 092002 (2015).

[52] V. Anastassopoulos *et al.* (CAST), New CAST Limit on the Axion-Photon Interaction, *Nature Phys.* **13**, 584 (2017), arXiv:1705.02290 [hep-ex].

[53] A. Caputo, G. Raffelt, and E. Vitagliano, Muonic boson limits: Supernova redux, *Phys. Rev. D* **105**, 035022 (2022).

[54] K. Hamaguchi, N. Nagata, K. Yanagi, and J. Zheng, Limit on the axion decay constant from the cooling neutron star in cassiopeia a, *Phys. Rev. D* **98**, 103015 (2018).

[55] D. Marsh, H. R. Russell, A. C. Fabian, B. R. McNamara, P. Nulsen, and C. S. Reynolds, A new bound on axion-like particles, *Journal of Cosmology and Astroparticle Physics* **2017** (12), 036.

[56] M. Meyer, M. Giannotti, A. Mirizzi, J. Conrad, and M. A. Sánchez-Conde, Fermi large area telescope as a galactic supernovae axionscope, *Phys. Rev. Lett.* **118**, 011103 (2017).

[57] M. Regis, M. Taoso, D. Vaz, J. Brinchmann, S. L. Zoutendijk, N. F. Bouché, and M. Steinmetz, Searching for light in the darkness: Bounds on alp dark matter with the optical muse-faint survey, *Physics Letters B* **814**, 136075 (2021).

[58] K. M. Backes, D. A. Palken, S. A. Kenany, B. M. Brubaker, S. B. Cahn, A. Droster, G. C. Hilton, S. Ghosh, H. Jackson, S. K. Lamoreaux, A. F. Leder, K. W. Lehnert, S. M. Lewis, M. Malnou, R. H. Maruyama, N. M. Rapidis, M. Simanovskaia, S. Singh, D. H. Speller, I. Urdinaran, L. R. Vale, E. C. van Assendelft, K. van Bibber, and H. Wang, A quantum enhanced search for dark matter axions, *Nature (London)* **590**, 238 (2021), arXiv:2008.01853 [quant-ph].

[59] D. Marsh, Axion cosmology, *Physics Reports* **643**, 1 (2016), axion cosmology.

[60] P. Sikivie, Experimental Tests of the “Invisible” Axion, *Phys. Rev. Lett.* **51**, 1415 (1983).

[61] L. B. Okun, Limits of electrodynamics: paraphotons?, *Sov. Phys. JETP* **56**, 502 (1982).

[62] A. Vilenkin, Particles and the universe, G. Lazarides and Q. Shafi (eds.), North Holland, Amsterdam , 133 (1986).

[63] P. Chen, Resonant photon-graviton conversion in EM fields: from earth to heaven, in *1st International Conference on Phenomenology of Unification: from Present to Future* (1994) pp. 379–395.

[64] F. Bastianelli, U. Nucamendi, C. Schubert, and V. M. Villanueva, Photon-graviton mixing in an electromagnetic field, *J. Phys. A* **41**, 164048 (2008), arXiv:0711.0992 [hep-th].

[65] A. D. Dolgov and D. Ejlli, Conversion of relic gravitational waves into photons in cosmological magnetic fields, *JCAP* **12**, 003, arXiv:1211.0500 [gr-qc].

[66] B. P. Abbott *et al.* (LIGO Scientific Collaboration and Virgo Collaboration), Observation of gravitational waves from a binary black hole merger, *Phys. Rev. Lett.* **116**, 061102 (2016).

[67] A. Ejlli, D. Ejlli, A. M. Cruise, G. Pisano, and H. Grote, Upper limits on the amplitude of ultra-high-frequency gravitational waves from graviton to photon conversion, *European Physical Journal C* **79**, 1032 (2019), arXiv:1908.00232 [gr-qc].

[68] T. Fujita, K. Kamada, and Y. Nakai, Gravitational waves from primordial magnetic fields via photon-graviton conversion, *Phys. Rev. D* **102**, 103501 (2020), arXiv:2002.07548 [astro-ph.CO].

[69] S. DePanfilis, A. C. Melissinos, B. E. Moskowitz, J. T. Rogers, Y. K. Semertzidis, W. U. Wuensch, H. J. Hallama, A. G. Prodell, W. B. Fowler, and F. A. Nezrick, Limits on the abundance and coupling of cosmic axions at $4.5 < m_a < 5.0 \mu\text{ev}$, *Phys. Rev. Lett.* **59**, 839 (1987).

[70] C. Hagmann, P. Sikivie, N. S. Sullivan, and D. B. Tanner, Results from a search for cosmic axions, *Phys. Rev. D* **42**, 1297 (1990).

[71] S. J. Asztalos, G. Carosi, C. Hagmann, D. Kinion, K. van Bibber, M. Hotz, L. J. Rosenberg, G. Rybka, J. Hoskins, J. Hwang, P. Sikivie, D. B. Tanner, R. Bradley, and J. Clarke, Squid-based microwave cavity search for dark-matter axions, *Phys. Rev. Lett.* **104**, 041301 (2010).

[72] L. Zhong, S. Al Kenany, K. M. Backes, B. M. Brubaker, S. B. Cahn, G. Carosi, Y. V. Gurevich, W. F. Kindel, S. K. Lamoreaux, K. W. Lehnert, S. M. Lewis, M. Malnou, R. H. Maruyama, D. A. Palken, N. M. Rapidis, J. R. Root, M. Simanovskaia, T. M. Shokair, D. H. Speller, I. Urdinaran, and K. A. van Bibber, Results from phase 1 of the haystac microwave cavity axion experiment, *Phys. Rev. D* **97**, 092001 (2018).

[73] Y. Lee, B. Yang, H. Yoon, M. Ahn, H. Park, B. Min, D. Kim, and J. Yoo, Searching for invisible axion dark matter with an 18 t magnet haloscope, *Phys. Rev. Lett.* **128**, 241805 (2022).

[74] H. Chang, J.-Y. Chang, Y.-C. Chang, Y.-H. Chang, Y.-H. Chang, C.-H. Chen, C.-F. Chen, K.-Y. Chen, Y.-F. Chen, W.-Y. Chiang, W.-C. Chien, H. T. Doan, W.-C. Hung, W. Kuo, S.-B. Lai, H.-W. Liu, M.-W. OuYang, P.-I. Wu, and S.-S. Yu, Taiwan axion search experiment with haloscope: Designs and operations, *Review of Scientific Instruments* **93**, 084501 (2022), <https://doi.org/10.1063/5.0098783>.

[75] B. Majorovits (MADMAX interest Group), MADMAX: A new road to axion dark matter detection, *J. Phys. Conf. Ser.* **1342**, 012098 (2017), arXiv:1712.01062 [physics.ins-det].

[76] M. Baryakhtar, J. Huang, and R. Lasenby, Axion and hidden photon dark matter detection with multilayer optical haloscopes, *Phys. Rev. D* **98**, 035006 (2018).

[77] J. De Miguel, A dark matter telescope probing the 6 to 60 GHz band, *Journal of Cosmology and Astroparticle Physics* **2021** (04), 075.

[78] R. N. Clarke and C. B. Rosenberg, Fabry-perot and open resonators at microwave and millimetre wave frequencies, 2-300 GHz, *Journal of Physics E: Scientific Instruments* **15**, 9 (1982).

[79] K. Renk, *Basics of Laser Physics: For Students of Science and Engineering*, Graduate Texts in Physics (Springer Berlin Heidelberg, 2012).

[80] N. Ismail, C. C. Kores, D. Geskus, and M. Pollnau, Fabry-pérot resonator: spectral line shapes, generic and related airy distributions, linewidths, finesse, and performance at low or frequency-dependent reflectivity, *Opt. Express* **24**, 16366 (2016).

[81] S. A. Bryan, T. E. Montroy, and J. E. Ruhl, Modeling dielectric half-wave plates for cosmic microwave background polarimetry using a mueller matrix formalism, *Appl. Opt.* **49**, 6313 (2010).

[82] R. Génova-Santos, J. A. R. Martín, R. Rebolo, A. Peláez-Santos, C. H. López-Carabal, S. Harper, R. A. Watson, M. Ashdown, R. B. Barreiro, B. Casappona, C. Dickinson, J. M. Diego, R. Fernández-Cobos, K. J. B. Grainge, C. M. Gutiérrez, D. Herranz, R. Hoyland, A. Lasenby, M. López-Caniego, E. Martínez-González, M. McCulloch, S. Melhuish, L. Piccirillo, Y. C. Perrott, F. Poidevin, N. Razavi-Ghods, P. F. Scott, D. Titterington, D. Tramonte, P. Vielva, and

R. Vignaga, QUIJOTE scientific results – I. Measurements of the intensity and polarisation of the anomalous microwave emission in the Perseus molecular complex, *Monthly Notices of the Royal Astronomical Society* **452**, 4169 (2015), <https://academic.oup.com/mnras/article-pdf/452/4/4169/18232343/stv1405.pdf>.

[83] M. D. Bird, I. R. Dixon, and J. Toth, Large, high-field magnet projects at the nfmfl, *IEEE Transactions on Applied Superconductivity* **25**, 1 (2015).

[84] H. Liebel, High-field superconducting magnets, in *High-Field MR Imaging*, edited by J. Hennig and O. Speck (Springer Berlin Heidelberg, Berlin, Heidelberg, 2012) pp. 7–25.

[85] Y. Lvovsky, E. W. Stautner, and T. Zhang, Novel technologies and configurations of superconducting magnets for MRI, *Superconductor Science Technology* **26**, 093001 (2013).

[86] C. Abel, S. Afach, N. J. Ayres, C. A. Baker, G. Ban, G. Bison, K. Bodek, V. Bondar, M. Burghoff, E. Chanel, Z. Chowdhuri, P.-J. Chiu, B. Clement, C. B. Crawford, M. Daum, S. Emmenegger, L. Ferraris-Bouchez, M. Fertl, P. Flaux, B. Franke, A. Fratangelo, P. Geltenbort, K. Green, W. C. Griffith, M. van der Grinten, Z. D. Grujić, P. G. Harris, L. Hayen, W. Heil, R. Henneck, V. Hélaine, N. Hild, Z. Hodge, M. Horras, P. Iaydjiev, S. N. Ivanov, M. Kasprzak, Y. Kermaidic, K. Kirch, A. Knecht, P. Knowles, H.-C. Koch, P. A. Koss, S. Komposch, A. Kozela, A. Kraft, J. Krempel, M. Kužniak, B. Lauss, T. Lefort, Y. Lemièvre, A. Leredde, P. Mohanmurthy, A. Mtchedlishvili, M. Musgrave, O. Naviliat-Cuncic, D. Pais, F. M. Piegsa, E. Pierre, G. Pignol, C. Plonka-Spehr, P. N. Prashanth, G. Quéméner, M. Rawlik, D. Rebreyend, I. Rienäcker, D. Ries, S. Rocca, G. Rogel, D. Rozpedzik, A. Schnabel, P. Schmidt-Wellenburg, N. Severijns, D. Shiers, R. Tavakoli Dinani, J. A. Thorne, R. Virot, J. Voigt, A. Weis, E. Wursten, G. Wyszynski, J. Zejma, J. Zenner, and G. Zsigmond, Measurement of the permanent electric dipole moment of the neutron, *Phys. Rev. Lett.* **124**, 081803 (2020).

[87] C. A. Baker, D. D. Doyle, P. Geltenbort, K. Green, M. G. D. van der Grinten, P. G. Harris, P. Iaydjiev, S. N. Ivanov, D. J. R. May, J. M. Pendlebury, J. D. Richardson, D. Shiers, and K. F. Smith, Improved experimental limit on the electric dipole moment of the neutron, *Phys. Rev. Lett.* **97**, 131801 (2006).

[88] H. Primakoff, Photoproduction of neutral mesons in nuclear electric fields and the mean life of the neutral meson, *Phys. Rev.* **81**, 899 (1951).

[89] J. E. Kim, Weak-interaction singlet and strong CP invariance, *Phys. Rev. Lett.* **43**, 103 (1979).

[90] M. A. Shifman, A. Vainshtein, and V. I. Zakharov, Can confinement ensure natural cp invariance of strong interactions, *Nuclear Physics* **166**, 493 (1980).

[91] M. Dine, W. Fischler, and M. Srednicki, A simple solution to the strong cp problem with a harmless axion, *Physics Letters B* **104**, 199 (1981).

[92] A. P. Zhitnitskii, Possible suppression of axion-hadron interactions, *Sov. J. Nucl. Phys. (Engl. Transl.); (United States)* **31:2**, (1980).

[93] K. Choi, S. H. Im, and C. S. Shin, Recent progress in the physics of axions and axion-like particles, *Annual Review of Nuclear and Particle Science* **71**, 225 (2021), <https://doi.org/10.1146/annurev-nucl-120720-031147>.

[94] F. Chadha-Day, J. Ellis, and D. J. E. Marsh, Axion dark matter: What is it and why now?, *Science Advances* **8**, eabj3618 (2022), <https://www.science.org/doi/pdf/10.1126/sciadv.abj3618>.

[95] A. A. Melcón *et al.* (CAST), First results of the CAST-RADES haloscope search for axions at $34.67 \mu\text{eV}$, *JHEP* **21**, 075, arXiv:2104.13798 [hep-ex].

[96] J. W. Foster, Y. Kahn, O. Macias, Z. Sun, R. P. Eatough, V. I. Kondratiev, W. M. Peters, C. Weniger, and B. R. Safdi, Green Bank and Effelsberg Radio Telescope Searches for Axion Dark Matter Conversion in Neutron Star Magnetospheres, *Phys. Rev. Lett.* **125**, 171301 (2020), arXiv:2004.00011 [astro-ph.CO].

[97] J. Darling, New Limits on Axionic Dark Matter from the Magnetar PSR J1745-2900, *Astrophys. J. Lett.* **900**, L28 (2020), arXiv:2008.11188 [astro-ph.CO].

[98] J. Darling, Search for Axionic Dark Matter Using the Magnetar PSR J1745-2900, *Phys. Rev. Lett.* **125**, 121103 (2020), arXiv:2008.01877 [astro-ph.CO].

[99] C. Boutan, M. Jones, B. H. LaRoque, N. S. Oblath, R. Cervantes, N. Du, N. Force, S. Kimes, R. Ottens, L. J. Rosenberg, G. Rybka, J. Yang, G. Carosi, N. Woollett, D. Bowring, A. S. Chou, R. Khatiwada, A. Sonnenschein, W. Wester, R. Bradley, E. J. Daw, A. Agrawal, A. V. Dixit, J. Clarke, S. R. O’Kelley, N. Crisosto, J. R. Gleason, S. Jois, P. Sikivie, I. Stern, N. S. Sullivan, D. B. Tanner, P. M. Harrington, and E. Lentz (ADMX Collaboration), Piezoelectrically tuned multimode cavity search for axion dark matter, *Phys. Rev. Lett.* **121**, 261302 (2018).

[100] D. Alesini, C. Braggio, G. Carugno, N. Crescini, D. D’Agostino, D. Di Gioacchino, R. Di Vora, P. Falferi, S. Gallo, U. Gambardella, C. Gatti, G. Iannone, G. Lamanna, C. Ligi, A. Lombardi, R. Mezzena, A. Ortolan, R. Pengo, N. Pompeo, A. Rettaroli, G. Ruoso, E. Silva, C. C. Speake, L. Taffarello, and S. Tocci, Galactic axions search with a superconducting resonant cavity, *Phys. Rev. D* **99**, 101101 (2019).

[101] Alesini *et al.*, Search for invisible axion dark matter of mass $m_a = 43 \mu\text{eV}$ with the quax- $a\gamma$ experiment, *Phys. Rev. D* **103**, 102004 (2021).

[102] B. T. McAllister, G. Flower, E. N. Ivanov, M. Goryachev, J. Bourhill, and M. E. Tobar, The organ experiment: An axion haloscope above 15 ghz, *Physics of the Dark Universe* **18**, 67 (2017).

[103] A. Quiskamp, B. T. McAllister, P. Altin, E. N. Ivanov, M. Goryachev, and M. E. Tobar, Direct search for dark matter axions excluding alp co-annihilation in the 63 to $67 \mu\text{eV}$ range with the organ experiment, *Science Advances* **8**, eabq3765 (2022), <https://www.science.org/doi/pdf/10.1126/sciadv.abq3765>.

[104] C. O’Hare, cajohare/axionlimits: Axionlimits, <https://cajohare.github.io/AxionLimits/> (2020).

[105] M. A. McCulloch, J. Grahn, S. J. Melhuish, P.-A. Nilsson, L. Piccirillo, J. Schleeh, and N. Wade Falk, Dependence of noise temperature on physical temperature for cryogenic low-noise amplifiers, *Journal of Astronomical Telescopes, Instruments, and Systems* **3**, 014003 (2017).

[106] J. Schleeh, J. Mateos, I. Íñiguez-de-la Torre, N. Wade Falk, P. Nilsson, J. Grahn, and A. Minnich, Phonon black-body radiation limit for heat dissipation in electronics, *Nature materials* **14**, 187–192 (2015).

[107] L. Di Luzio, F. Mescia, and E. Nardi, Redefining the Axion Window, *Phys. Rev. Lett.* **118**, 031801 (2017),

arXiv:1610.07593 [hep-ph].

[108] See Supplemental Material at [URL will be inserted by publisher] for a numerical estimate of DALI sensitivity by means of a Monte Carlo simulation that shows good agreement with the naive calculation included in the Main Letter.

[109] A. D. Linde, Axions in inflationary cosmology, *Phys. Lett. B* **259**, 38 (1991).

[110] T. Hiramatsu, M. Kawasaki, K. Saikawa, and T. Sekiguchi, Production of dark matter axions from collapse of string-wall systems, *Phys. Rev. D* **85**, 105020 (2012), [Erratum: *Phys. Rev. D* **86**, 089902 (2012)], arXiv:1202.5851 [hep-ph].

[111] S. M. Barr and J. E. Kim, New Confining Force Solution of the QCD Axion Domain-Wall Problem, *Phys. Rev. Lett.* **113**, 241301 (2014), arXiv:1407.4311 [hep-ph].

[112] R. Sato, F. Takahashi, and M. Yamada, Unified origin of axion and monopole dark matter, and solution to the domain-wall problem, *Phys. Rev. D* **98**, 043535 (2018).

[113] A. Ringwald and K. Saikawa, Axion dark matter in the post-inflationary peccei-quinn symmetry breaking scenario, *Phys. Rev. D* **93**, 085031 (2016).

[114] T. Hiramatsu, M. Kawasaki, and K. Saikawa, Evolution of string-wall networks and axionic domain wall problem, *Journal of Cosmology and Astroparticle Physics* **2011** (08), 030.

[115] M. Kawasaki, T. T. Yanagida, and K. Yoshino, Domain wall and isocurvature perturbation problems in axion models, *Journal of Cosmology and Astroparticle Physics* **2013** (11), 030.

[116] K. Harigaya and M. Kawasaki, Qcd axion dark matter from long-lived domain walls during matter domination, *Physics Letters B* **782**, 1 (2018).

[117] C. A. J. O'Hare, G. Pierobon, J. Redondo, and Y. Y. Y. Wong, Simulations of axionlike particles in the post-inflationary scenario, *Phys. Rev. D* **105**, 055025 (2022).

[118] M. Buschmann, J. W. Foster, A. Hook, A. Peterson, D. E. Willcox, W. Zhang, and B. R. Safdi, Dark matter from axion strings with adaptive mesh refinement, *Nature Communications* **13**, 1049 (2022), arXiv:2108.05368 [hep-ph].

[119] G. G. Raffelt and D. S. P. Dearborn, Bounds on hadronic axions from stellar evolution, *Phys. Rev. D* **36**, 2211 (1987).

[120] G. G. Raffelt, Particle physics from stars, *Ann. Rev. Nucl. Part. Sci.* **49**, 163 (1999), arXiv:hep-ph/9903472.

[121] N. Viaux, M. Catelan, P. B. Stetson, G. Raffelt, J. Redondo, A. A. R. Valcarce, and A. Weiss, Neutrino and axion bounds from the globular cluster M5 (NGC 5904), *Phys. Rev. Lett.* **111**, 231301 (2013), arXiv:1311.1669 [astro-ph.SR].

[122] A. Ayala, I. Domínguez, M. Giannotti, A. Mirizzi, and O. Straniero, Revisiting the bound on axion-photon coupling from Globular Clusters, *Phys. Rev. Lett.* **113**, 191302 (2014), arXiv:1406.6053 [astro-ph.SR].

[123] M. M. Miller Bertolami, B. E. Melendez, L. G. Althaus, and J. Isern, Revisiting the axion bounds from the Galactic white dwarf luminosity function, *JCAP* **10**, 069, arXiv:1406.7712 [hep-ph].

[124] T. Fischer, S. Chakraborty, M. Giannotti, A. Mirizzi, A. Payez, and A. Ringwald, Probing axions with the neutrino signal from the next galactic supernova, *Phys. Rev. D* **94**, 085012 (2016), arXiv:1605.08780 [astro-ph.HE].

[125] P. Carenza, T. Fischer, M. Giannotti, G. Guo, G. Martínez-Pinedo, and A. Mirizzi, Improved axion emissivity from a supernova via nucleon-nucleon bremsstrahlung, *JCAP* **10** (10), 016, [Erratum: *JCAP* **05**, E01 (2020)], arXiv:1906.11844 [hep-ph].

[126] L. B. Leinson, Axion mass limit from observations of the neutron star in Cassiopeia A, *JCAP* **08**, 031, arXiv:1405.6873 [hep-ph].

[127] J. Keller and A. Sedrakian, Axions from cooling compact stars, *Nucl. Phys. A* **897**, 62 (2013), arXiv:1205.6940 [astro-ph.CO].

[128] M. Giannotti, I. G. Irastorza, J. Redondo, A. Ringwald, and K. Saikawa, Stellar Recipes for Axion Hunters, *JCAP* **10**, 010, arXiv:1708.02111 [hep-ph].

[129] O. Straniero, C. Pallanca, E. Dalessandro, I. Dominguez, F. R. Ferraro, M. Giannotti, A. Mirizzi, and L. Piersanti, The RGB tip of galactic globular clusters and the revision of the axion-electron coupling bound, *Astron. Astrophys.* **644**, A166 (2020), arXiv:2010.03833 [astro-ph.SR].

[130] L. D. Luzio, M. Fedele, M. Giannotti, F. Mescia, and E. Nardi, Stellar evolution confronts axion models (2021), arXiv:2109.10368 [hep-ph].

[131] J. De Miguel and C. Otani, Superdense beaming of axion dark matter in the vicinity of the light cylinder of pulsars, *Journal of Cosmology and Astroparticle Physics* **2022** (08), 026.

[132] J. De Miguel and C. Otani, Axion-photon multimesenger astronomy with giant flares, *Phys. Rev. D* **106**, L041302 (2022b).

[133] J. De Miguel, Retuning the radio astronomical search for axion dark matter with neutron stars, arXiv e-prints, arXiv:2301.10144 (2023), arXiv:2301.10144 [hep-ph].

[134] P. Arias, D. Cadamuro, M. Goodsell, J. Jaeckel, J. Redondo, and A. Ringwald, WISPy Cold Dark Matter, *JCAP* **06**, 013, arXiv:1201.5902 [hep-ph].

[135] J. Suzuki, Y. Inoue, T. Horie, and M. Minowa, Hidden photon CDM search at Tokyo, in *11th Patras Workshop on Axions, WIMPs and WISPs* (2015) pp. 145–148, arXiv:1509.00785 [hep-ex].

[136] C. Boutan *et al.* (ADMX), Piezoelectrically Tuned Multimode Cavity Search for Axion Dark Matter, *Phys. Rev. Lett.* **121**, 261302 (2018), arXiv:1901.00920 [hep-ex].

[137] P. Brun, L. Chevalier, and C. Flouzat, Direct Searches for Hidden-Photon Dark Matter with the SHUKET Experiment, *Phys. Rev. Lett.* **122**, 201801 (2019), arXiv:1905.05579 [hep-ex].

[138] A. V. Dixit, S. Chakram, K. He, A. Agrawal, R. K. Naik, D. I. Schuster, and A. Chou, Searching for Dark Matter with a Superconducting Qubit, *Phys. Rev. Lett.* **126**, 141302 (2021), arXiv:2008.12231 [hep-ex].

[139] R. Cervantes *et al.*, ADMX-Orpheus first search for 70 μ eV dark photon dark matter: Detailed design, operations, and analysis, *Phys. Rev. D* **106**, 102002 (2022), arXiv:2204.09475 [hep-ex].

[140] R. Cervantes *et al.*, Search for 70 μ eV Dark Photon Dark Matter with a Dielectrically Loaded Multiwavelength Microwave Cavity, *Phys. Rev. Lett.* **129**, 201301 (2022), arXiv:2204.03818 [hep-ex].

[141] A. Caputo, A. J. Millar, C. A. J. O'Hare, and E. Vitagliano, Dark photon limits: A handbook, *Phys. Rev. D* **104**, 095029 (2021), arXiv:2105.04565 [hep-ph].

[142] D. Horns, J. Jaeckel, A. Lindner, A. Lobanov, J. Redondo, and A. Ringwald, Searching for WISPy Cold Dark Matter with a Dish Antenna, *JCAP* **04**, 016, arXiv:1212.2970 [hep-ph].

[143] C. J. Hogan and M. J. Rees, AXION MINICLUSTERS, *Phys. Lett. B* **205**, 228 (1988).

[144] C. A. O’Hare and A. M. Green, Axion astronomy with microwave cavity experiments, *Physical Review D* **95**, 063017 (2017).

[145] S. Knirck, A. J. Millar, C. A. J. O’Hare, J. Redondo, and F. D. Steffen, Directional axion detection, *Journal of Cosmology and Astroparticle Physics* **2018** (11), 051, arXiv:1806.05927 [astro-ph.CO].

[146] C. A. J. O’Hare, C. McCabe, N. W. Evans, G. Myeong, and V. Belokurov, Dark matter hurricane: Measuring the s1 stream with dark matter detectors, *Phys. Rev. D* **98**, 103006 (2018).

[147] H. Fischer, X. Liang, Y. Semertzidis, A. Zhitnitsky, and K. Zioutas, New mechanism producing axions in the AQN model and how the CAST can discover them, *Phys. Rev. D* **98**, 043013 (2018), arXiv:1805.05184 [hep-ph].

[148] X. Liang and A. Zhitnitsky, Gravitationally bound axions and how one can discover them, *Phys. Rev. D* **99**, 023015 (2019), arXiv:1810.00673 [hep-ph].

[149] X. Liang, A. Mead, M. S. R. Siddiqui, L. Van Waerbeke, and A. Zhitnitsky, Axion Quark Nugget Dark Matter: Time Modulations and Amplifications, *Phys. Rev. D* **101**, 043512 (2020), arXiv:1908.04675 [astro-ph.CO].

[150] D. Budker, V. V. Flambaum, X. Liang, and A. Zhitnitsky, Axion Quark Nuggets and how a Global Network can discover them, *Phys. Rev. D* **101**, 043012 (2020), arXiv:1909.09475 [hep-ph].

[151] B. R. Patla, R. J. Nemiroff, D. H. H. Hoffmann, and K. Zioutas, Flux enhancement of slow-moving particles by sun or jupiter: Can they be detected on earth?, *The Astrophysical Journal* **780**, 158 (2013).

[152] A. J. Millar, J. Redondo, and F. D. Steffen, Dielectric haloscopes: sensitivity to the axion dark matter velocity, *JCAP* **10**, 006, [Erratum: *JCAP* 05, E02 (2018)], arXiv:1707.04266 [hep-ph].

[153] P. W. Gorham, J. Nam, A. Romero-Wolf, S. Hoover, P. Allison, O. Banerjee, J. J. Beatty, K. Belov, D. Z. Besson, W. R. Binns, V. Bugaev, P. Cao, C. Chen, P. Chen, J. M. Clem, A. Connolly, B. Dailey, C. Deaconu, L. Cremonesi, P. F. Dowkontt, M. A. DuVernois, R. C. Field, B. D. Fox, D. Goldstein, J. Gordon, C. Hast, C. L. Hebert, B. Hill, K. Hughes, R. Hupe, M. H. Israel, A. Javaid, J. Kowalski, J. Lam, J. G. Learned, K. M. Liewer, T. C. Liu, J. T. Link, E. Lusczek, S. Matsuno, B. C. Mercurio, C. Miki, P. Miočinović, M. Mottram, K. Mulrey, C. J. Naudet, J. Ng, R. J. Nichol, K. Palladino, B. F. Rauch, K. Reil, J. Roberts, M. Rosen, B. Rotter, J. Russell, L. Ruckman, D. Saltzberg, D. Seckel, H. Schoorlemmer, S. Stafford, J. Stockham, M. Stockham, B. Strutt, K. Tatem, G. S. Varner, A. G. Vieregg, D. Walz, S. A. Wissel, and F. Wu (ANITA Collaboration), Characteristics of four upward-pointing cosmic-ray-like events observed with anita, *Phys. Rev. Lett.* **117**, 071101 (2016).

[154] P. W. Gorham *et al.* (ANITA), Observation of an Unusual Upward-going Cosmic-ray-like Event in the Third Flight of ANITA, *Phys. Rev. Lett.* **121**, 161102 (2018), arXiv:1803.05088 [astro-ph.HE].

[155] I. Esteban, J. Lopez-Pavon, I. Martinez-Soler, and J. Salvado, Looking at the axionic dark sector with ANITA, *Eur. Phys. J. C* **80**, 259 (2020), arXiv:1905.10372 [hep-ph].

[156] M. Gertsenshtain, Resonance of light and gravitational waves, *Soviet Physics JETP. Fiz.* **14**, 84 (1962).

[157] G. Raffelt and L. Stodolsky, Mixing of the photon with low-mass particles, *Phys. Rev. D* **37**, 1237 (1988).

[158] J. A. R. Cembranos, M. C. Diaz, and P. Martin-Moruno, Graviton-photon oscillation in alternative theories of gravity, *Class. Quant. Grav.* **35**, 205008 (2018), arXiv:1806.11020 [gr-qc].

[159] J. A. Marck and J. P. Lasota, eds., *Relativistic gravitation and gravitational radiation. Proceedings, School of Physics, Les Houches, France, September 26-October 6, 1995* (Cambridge Univ.Pr., Cambridge, UK, 1997).

[160] M. Maggiore, Gravitational wave experiments and early universe cosmology, *Phys. Rept.* **331**, 283 (2000), arXiv:gr-qc/9909001.

[161] M. Servin and G. Brodin, Resonant interaction between gravitational waves, electromagnetic waves and plasma flows, *Phys. Rev. D* **68**, 044017 (2003), arXiv:gr-qc/0302039.

[162] G. S. Bisnovatyi-Kogan and V. N. Rudenko, Very high frequency gravitational wave background in the universe, *Class. Quant. Grav.* **21**, 3347 (2004), arXiv:gr-qc/0406089.

[163] C. Clarkson and S. S. Seahra, A gravitational wave window on extra dimensions, *Class. Quant. Grav.* **24**, F33 (2007), arXiv:astro-ph/0610470.

[164] A. Ejlli, D. Ejlli, A. M. Cruise, G. Pisano, and H. Grote, Upper limits on the amplitude of ultra-high-frequency gravitational waves from graviton to photon conversion, *Eur. Phys. J. C* **79**, 1032 (2019), arXiv:1908.00232 [gr-qc].

[165] A. Ito, T. Ikeda, K. Miuchi, and J. Soda, Probing GHz gravitational waves with graviton-magnon resonance, *Eur. Phys. J. C* **80**, 179 (2020), arXiv:1903.04843 [gr-qc].

[166] A. S. Chou, R. Gustafson, C. Hogan, B. Kamai, O. Kwon, R. Lanza, S. L. Larson, L. McCuller, S. S. Meyer, J. Richardson, C. Stoughton, R. Tomlin, R. Weiss, and Holometer Collaboration, MHz gravitational wave constraints with decameter Michelson interferometers, *Phys. Rev. D* **95**, 063002 (2017), arXiv:1611.05560 [astro-ph.IM].

[167] A. M. Cruise and R. M. J. Ingleby, A prototype gravitational wave detector for 100-MHz, *Class. Quant. Grav.* **23**, 6185 (2006).

[168] A. Nishizawa *et al.*, Laser-interferometric Detectors for Gravitational Wave Background at 100 MHz: Detector Design and Sensitivity, *Phys. Rev. D* **77**, 022002 (2008), arXiv:0710.1944 [gr-qc].

[169] T. Akutsu *et al.*, Search for a stochastic background of 100-MHz gravitational waves with laser interferometers, *Phys. Rev. Lett.* **101**, 101101 (2008), arXiv:0803.4094 [gr-qc].

[170] R. Ballou *et al.* (OSQAR), New exclusion limits on scalar and pseudoscalar axionlike particles from light shining through a wall, *Phys. Rev. D* **92**, 092002 (2015), arXiv:1506.08082 [hep-ex].

[171] K. Ehret *et al.*, New ALPS Results on Hidden-Sector Lightweights, *Phys. Lett. B* **689**, 149 (2010), arXiv:1004.1313 [hep-ex].

- [172] R. H. Dicke, The measurement of thermal radiation at microwave frequencies, *Review of Scientific Instruments* **17**, 268 (1946), <https://doi.org/10.1063/1.1770483>.
- [173] G. Aad *et al.* (ATLAS), Observation of a new particle in the search for the Standard Model Higgs boson with the ATLAS detector at the LHC, *Phys. Lett. B* **716**, 1 (2012), arXiv:1207.7214 [hep-ex].
- [174] S. Chatrchyan *et al.* (CMS), Observation of a New Boson at a Mass of 125 GeV with the CMS Experiment at the LHC, *Phys. Lett. B* **716**, 30 (2012), arXiv:1207.7235 [hep-ex].
- [175] S. Chatrchyan *et al.* (CMS), Observation of a New Boson with Mass Near 125 GeV in pp Collisions at $\sqrt{s} = 7$ and 8 TeV, *JHEP* **06**, 081, arXiv:1303.4571 [hep-ex].
- [176] B. M. Brubaker, L. Zhong, S. K. Lamoreaux, K. W. Lehnert, and K. A. van Bibber, HAYSTAC axion search analysis procedure, *Phys. Rev. D* **96**, 123008 (2017).

**Discovery prospects with the Dark-photons
& Axion-Like particles Interferometer
—part I**

Supplementary Material

Javier De Miguel and Juan F. Hernández-Cabrera

In this supplementary material we recompute the sensitivity of DALI to Galactic axion dark matter by means of a Monte Carlo simulation, for which we will mainly follow [103, 176]. The input data consists of M individual spectra containing 2^N bins each generated synthetically. First, an average baseline is estimated by applying a Savitzky–Golay (SG) filter with a window size $W = 3001$ and a polynomial degree $d = 2$ to the average of all spectra. The average spectrum is then divided by the estimated baseline. Bins potentially compromised by intermediate frequency (IF) interferences are identified as any bin deviating more than 4.5σ from the average as well as 3 bins to each side; the values of these bins are iteratively replaced by randomly generated values drawn from a Gaussian distribution with the same average and standard deviation as the values of the average spectrum until no further compromised bins are identified. The corresponding bins of the individual spectra are also replaced with random values in the same manner. Bins potentially compromised by spurious radio frequency (RF) interference are identified in individual spectra as any bin deviating more than several sigma from the average, the threshold being an arbitrary value that is established based on the exclusion sector to be considered. Their values are iteratively replaced by randomly generated values drawn from a Gaussian distribution until no further RF interferences are found. The spectra are individually normalised to their estimated baseline, which is obtained by means of a SG filter with the same parameters as before, to get the processed spectra. Processed spectra are now rescaled by the expected power boost at each frequency to calculate the rescaled spectra, namely

$$\delta_{ij}^s = \frac{\delta_{ij}^p}{\beta_{ij}^2}, \quad (\text{S1})$$

where δ is the value of a bin, i is the index of a spectrum among all spectra, j is the index of a bin within a spectrum and β_{ij}^2 is the power boost provided by the resonator at each bin. The superscripts s and p represent the rescaled and the processed spectra, respectively. The standard deviation of each bin is given by

$$\sigma_{ij}^s = \frac{\sigma_i^p}{\beta_{ij}^2}. \quad (\text{S2})$$

The rescaled spectra are then combined into a stacked spectrum. The RF bins corresponding to a single IF bin—i.e., non-overlapping bands—are copied directly onto the stacked spectrum; RF bins in overlapping bands are combined by means of a maximum likelihood (ML) weighted sum where the weights w_{ijk} are calculated as

$$w_{ijk} = \frac{(\sigma_{ij}^s)^{-2}}{\sum_{i'} \sum_{j'} (\sigma_{i'j'}^s)^{-2}}, \quad (\text{S3})$$

where k is the index of the stacked spectrum. The prime notation in the denominator is to be interpreted as a sum across all pairs i, j corresponding to a bin k . The stacked spectrum can then be processed as

$$\delta_k^c = \sum_{i'} \sum_{j'} w_{ijk} \delta_{ij}^s \quad (\text{S4})$$

in the overlapping bands. The standard deviation of each stacked spectrum bin is calculated as

$$\sigma_k^c = \sqrt{\sum_{i'} \sum_{j'} w_{ijk}^2 (\delta_{ij}^s)^2}. \quad (\text{S5})$$

Now the rebinned spectrum is obtained by merging neighbouring bins of the stacked spectrum in non-overlapping segments of a length equal to K_r bins. Let $D_k^c = \delta_k^c (\sigma_k^c)^{-2}$ and $R_k^c = (\sigma_k^c)^{-1}$. The rebinned spectrum is obtained from

$$D_\ell^r = \sum_{k=(\ell-1)K_r+1}^{k=\ell K_r} D_k^c \quad (\text{S6})$$

and

$$R_\ell^r = \sqrt{\sum_{k=(\ell-1)K_r+1}^{k=\ell K_r} (R_k^c)^2}, \quad (\text{S7})$$

where ℓ is the index of the rebinned spectrum. The grand spectrum is obtained from a ML weighted sum taking into account the expected power spectral density or line shape $S_a(\nu)$ of the axion-induced signal. In this implementation, we have considered

$$S_a(\nu) = K \sqrt{\nu - \nu_a} \exp\left(-\frac{3(\nu - \nu_a)}{\nu_a \frac{\langle v_a^2 \rangle}{c^2}}\right), \quad (\text{S8})$$

at which K is a constant added to scale $S_a(\nu)$ to its expected power. The weights are calculated by integrating over segments of $S_a(\nu)$ with a length of K_r bins given a misalignment $\delta\nu_r$, according to

$$L_q(\delta\nu_r) = K_g \int_{\nu_a + \delta\nu_r + (q-1)K_r \Delta\nu_b}^{\nu_a + \delta\nu_r + qK_r \Delta\nu_b} S_a(\nu) d\nu, \quad (\text{S9})$$

where q is an index running from 1 up to K_g —the length of the grand spectrum ML sum—and $\Delta\nu_b$ is the bin width of the original spectra. It should be noted that the lengths K_r and K_g must be chosen such that the axion width, $\Delta\nu$, is, approximately, $K_r K_g$ bins wide. The spectral density function $S_a(\nu)$ has a full width half maximum of about $5 \times 10^{-7} \nu_a$ if a value of $(270 \text{ km/s})^2$ is considered for $\langle v_a^2 \rangle$ in a Maxwell–Boltzmann distribution [176]. In this procedure, we have considered an axion width equal to ~ 1.5 times the full width half maximum of $S_a(\nu)$. The misalignment is defined over a range given by

$$-z K_r \Delta\nu_b \leq \delta\nu_r \leq (1-z) K_r \Delta\nu_b \quad (\text{S10})$$

for $0 \leq z \leq 1$. The value of z must be set such that the sum $\sum_q L_q / K_g$ yields a larger value than the one obtained if the sum limits were shifted by 1 up or down for all $\delta\nu_r$. The weights \bar{L}_q are obtained by averaging out $L_q(\delta\nu_r)$ over the range of $\delta\nu_r$. The grand spectrum is now calculated as

$$D_\ell^g = \sum_q D_{\ell+q-1}^r \bar{L}_q, \quad (\text{S11})$$

and

$$R_\ell^g = \sqrt{\sum_q (R_{\ell+q-1}^r \bar{L}_q)^2}. \quad (\text{S12})$$

The normalised spectrum is obtained as $\delta_\ell^g / \sigma_\ell^g = D_\ell^g / R_\ell^g$. In order to account for filter-induced correlations among bins, the standard deviation, ξ , of the normalised grand spectrum is calculated, from which a corrected grand spectrum standard deviation $\tilde{\sigma}_\ell^g = \sigma_\ell^g / \xi$ is obtained. The output of this method, which is the normalised and corrected grand spectrum, is calculated as $\delta_\ell^g / \tilde{\sigma}_\ell^g$. An exclusion sector determined by the bins exceeding a threshold Θ for an arbitrary confidence level (CL) can be established, $\Theta = \text{SNR} - \Phi^{-1}(\text{CL})$, Φ being the cumulative distribution function of the standard normal distribution.

In Fig. S1, we report the result of a simulation after calculating 10,000 iterations. In each iteration, raw bins have been generated as random numbers in each spectrum drawn from a Gaussian distribution with mean $\mu = k_B T_{\text{sys}} \Delta\nu_b$ and deviation $\sigma = k_B T_{\text{sys}} \Delta\nu_b / \sqrt{t \Delta\nu_b}$ [172], scaled by the power boost curve [77]. An artificially generated discrete axion-induced signal has been inserted to one of the spectra as $S_{a,ij} \approx \Delta\nu_b S_a(\nu_{ij})$, which is successfully flagged. The resulting spectra are introduced as an input to the analysis procedure and the value of the output in a window of 150 bins at each side of the bin where the axion signal was inserted has been recorded. An instantaneous scanning bandwidth of 50 MHz has been considered, effective integration time is set to five days per subspectrum, and an array size of 2^{18} has been considered resulting in a bin width $\Delta\nu_b \simeq 190.7$ Hz. A total of $M = 2$ spectra with an overlap of 5 MHz have been considered around a central frequency of about 24.2 GHz, where the synthetic axion signal has been injected with $g_{a\gamma\gamma} \simeq 1.5 \times 10^{-14} \text{ GeV}^{-1}$, which corresponds to a DFSZ I axion of 100 μeV mass. Since an axion width of approximately 90 bins is expected at this frequency, $K_r = 7$ and $K_g = 14$ have been considered, for which the value $z = 0.51$ has been numerically found to best fit the requirements in Eq. S11 and Eq. S12. The weights, \bar{L}_q , have been calculated for $\nu_a \simeq 24.2$ GHz, but any frequency in the scan range would be suitable given that variations of $S_a(\nu)$ along a series of M subspectra tend to be negligible.

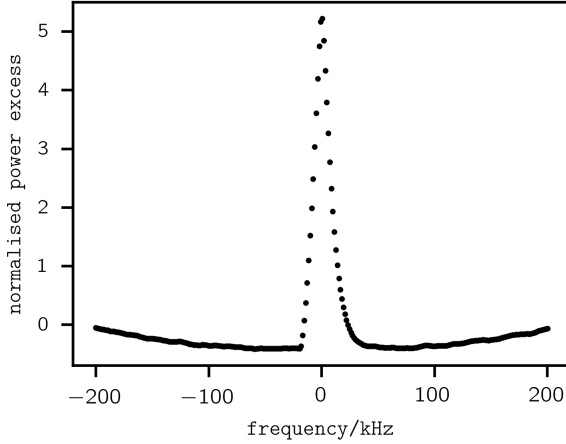


FIG. S1. Sensitivity calculation. The average value of the normalised corrected grand spectrum, $\delta_\ell^g/\tilde{\sigma}_\ell^g$, in a window of 150 bins to each side of the frequency where a synthetic axion signal has been injected is represented. The peak value (5.217) is to be interpreted as the SNR of the axion-induced signal. The distributions of the values of all bins of the analysed window have a standard deviation close to 1. The ripple around the peak is an artifact of the filtering. The abscissa axis has been scaled by K_r to account for the rebinning.